Supplementary Material

Discovery of Potent Myeloid Cell Leukemia-1 (Mcl-1) Inhibitors that Demonstrate *in vivo* Activity in Mouse Xenograft Models of Human Cancer

Taekyu Lee[1], Plamen P. Christov[2], Subrata Shaw[1], James C. Tarr[1], Bin Zhao[1], Nagarathanam Veerasamy[1], Kyu Ok Jeon[1], Jonathan J. Mills[1], Zhiguo Bian[1], John L. Sensintaffar[1], Allison L. Arnold[1], Stuart A. Fogarty[1], Evan Perry[1], Haley E. Ramsey[3], Rebecca S. Cook[4], Melinda Hollingshead[5], Myrtle Davis Millin[5], Kyung-min Lee[6], Brian Koss[7], Amit Budhraja[7], Joseph T. Opferman[7], Kwangho Kim[2], Carlos L. Arteaga[6], William J. Moore[8], Edward T. Olejniczak[1], Michael R. Savona[3] and Stephen W. Fesik[1]*

1. Department of Biochemistry, Vanderbilt University School of Medicine, 2215 Garland Avenue, 607 Light Hall, Nashville, Tennessee 37232-0146, USA

2. Chemical Synthesis Core, Vanderbilt Institute of Chemical Biology, Vanderbilt University, Nashville, Tennessee 37232, USA

3. Department of Medicine, Vanderbilt-Ingram Cancer Center, Nashville, Tennessee 37232, USA

4. Department of Cell and Developmental Biology, Vanderbilt University School of Medicine, Nashville, Tennessee 37232, USA

5. National Cancer Institute, Bethesda, MD, 20892, USA

6. Department of Hematology and Oncology, Vanderbilt University School of Medicine, Nashville, Tennessee 37232, USA

7. Department of Cell and Molecular Biology, St. Jude Children's Research Hospital, Memphis, TN 38105, USA

8. Leidos Biomedical Research, Frederick National Laboratory for Cancer Research, Frederick, MD 21701, USA

Table of Content

S1. X-ray Data Collection and Refinement Statistics (**42**)

S2. Evaluation of Mcl-1 Inhibitors with Proliferation Assay in Hematologic Cell Line Panel; Comparison to MS-1 Activity

S3. Additional Data for Dosing Compound **42** in HCC-1187 Xenograft Model

S4. Additional Data for Co-Dosing Experiments with **42** in HCC-1187 Xenograft Model

S5. Screening of compounds **35**-**43** in Mcl-1 sensitive cell line panel

S6. HPLC-MS traces for compounds **6**-**43**

S1.

*X-Ray Data collection and refinement statistics for **42***

Table 1 Data collection and refinement statistics

	Comp. **42**
Data collection	
Space group	$P2_1$
Cell dimensions	
a, *b*, *c* (Å)	39.33, 135.94, 60.05
α, β, γ (°)	90.00, 95.95, 90.00
Resolution (Å)	1.85 (1.85-1.88) *
R_{sym} or R_{merge}	0.04/0.05 (0.34/0.36)
$I / \sigma I$	23.76 (2.27)
Completeness (%)	80.0 (70.3)
Redundancy	3.9 (2.7)
Refinement	
Resolution (Å)	1.85-30.0
No. reflections	42686
R_{work} / R_{free}	0.17/0.21
No. atoms	
Protein	5396
Ligand	200
Water	424
B-factors	(Ask for input)
Protein	35
Ligand	23
Water	28
R.m.s. deviations	
Bond lengths (Å)	0.006
Bond angles (°)	0.79

*Number of xtals for each structure should be noted in footnote. *Values in parentheses are for highest-resolution shell.

[AU: Equations defining various *R*-values are standard and hence are no longer defined in the footnotes.]
[AU: Ramachandran statistics should be in Methods section at the end of Refinement subsection.]
[AU: Wavelength of data collection, temperature and beamline should all be in Methods section.]

S2. Evaluation of Mcl-1 Inhibitors with Proliferation Assay in Hematologic Cell Line Panel; Comparison to MS-1 Activity

Methods: Intracellular BH3 (iBH3) profiling

The synthetic peptide for MS-1 (ac-RPEIWMTQGLRRLGDEINAYYAR-NH_2), was purchased (Genscript). Cytochrome c loss was measured by iBH3 profiling as described earlier (Pan, R.; Hogdal, L. J., et al. *Cancer Discov*. **2014**, *4*, 362-375). Following cell fixation and cell quenching, cells were stained with of 1:100 dilution of anti-cytochrome c –Alexa647 (clone 6H2.B4; #612310, Biolegend) in a 10X staining buffer (20% FBS, 10% BSA, 1% Saponin, 3 mM sodium azide in PBS) to measure cytochrome c loss. Cytochrome c retention was measured on BD LSRII after overnight incubation with antibody and cytochrome c retention was measured using the following equation:

Cytochrome c loss = 100 – (% of cells within cytochrome c retention gate)

Figure 1: In panels A, B we show the activity of compound **42** against a panel of hematologic cell lines. In the proliferation experiments, we see differential sensitivity in the various cell lines, which is consistent with different levels of cell line priming to apoptosis. To test this hypothesis, we compared the cytochrome c release caused by **42** in iBH3 profiling experiments (1C) to that produced by the Mcl-1 specific MS-1 peptide in the same panel of hematologic cell lines show in the proliferation studies. In general we find that cell lines that have greater percent cytochrome c release after dosing with the Mcl-1 selective MS-1 peptide have a similar cytochrome c release when dosed with the same concentration of compound **42**. Cell lines with high cytochrome c release in this experiment also have lower GI_{50} in the proliferation studies.

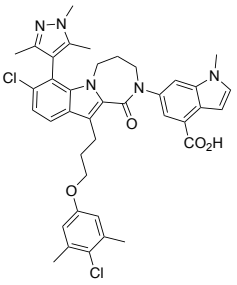

VU0659158

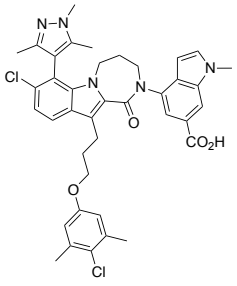

VU0659159

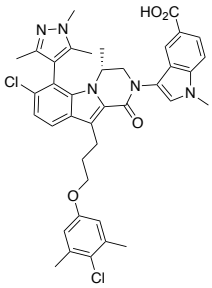

Compound 42/VU0661013

A.

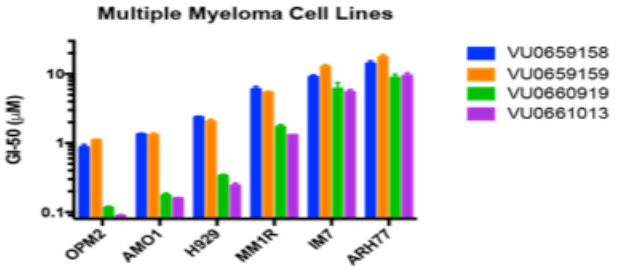

B.

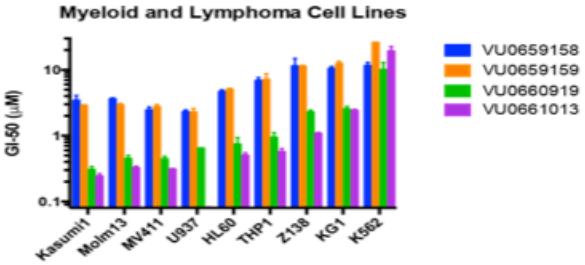

C.

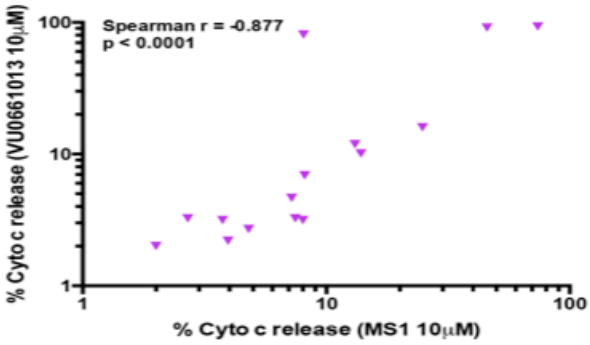

S3. Additional Data for Dosing Compound 42 in HCC-1187 Xenograft Model

S3 Figure Methods, Immunohistochemistry Analysis

Tumors were resected from mice, fixed in 10% neutral buffered formalin (Sigma), and imaged in whole mount prior to paraffin embedding by the Histopathology Shared Resource of the VICC Breast Cancer SPORE. Sections were rehydrated, followed by trypsin-mediated antigen retrieval. Sections were blocked in 5% normal goat serum. IHC on paraffin-embedded sections was performed using primary antibody against cleaved caspase-3 (clone 5AE1 diluted at 1:500, Cell Signaling Technology). Immunodetection was performed using Vectastain (Vector Laboratories) according to the manufacturer's directions. Photomicrographs acquired on an Olympus CK40 inverted microscope through an Optronics DEI-750C charge-coupled-device video camera using CellSens capture software.

Figure S3. Further characterization of tumor growth studies of HCC-1187 xenographs. A) Tumors extracted from animals at end of study (B) Immunohistochemistry analysis of caspase activation in tumors after 14 days of dosing (100 mg/kg IP) or untreated controls UTX (C) Average weight change of animals over course of study.

A.

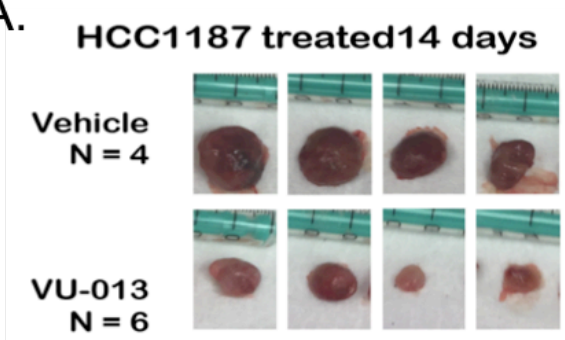
HCC1187 treated14 days
Vehicle
N = 4
VU-013
N = 6

B.

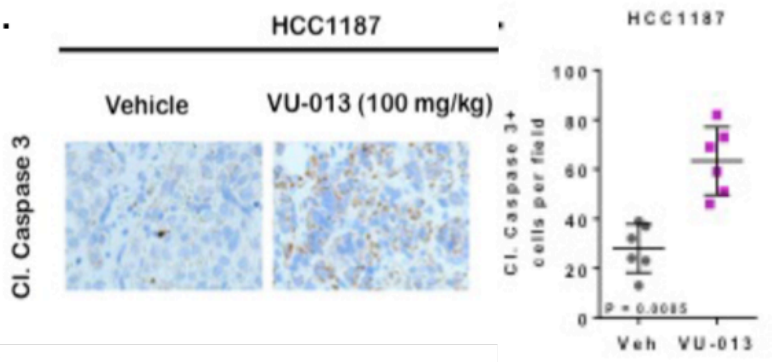
HCC1187
Vehicle
VU-013 (100 mg/kg)
Cl. Caspase 3
HCC1187
Cl. Caspase 3+ cells per field
100
80
60
40
20
0
P = 0.0085
Veh
VU-013

C.

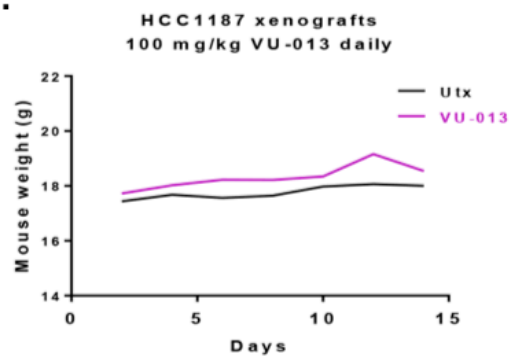
HCC1187 xenografts
100 mg/kg VU-013 daily
Utx
VU-013
Mouse weight (g)
22
20
18
16
14
0
5
10
15
Days

S4. Additional Data for Co-Dosing Experiments with 42 in HCC-1187 Xenograft Model

Figure S4. *Co-dosing studies HCC-1187 TNBC*

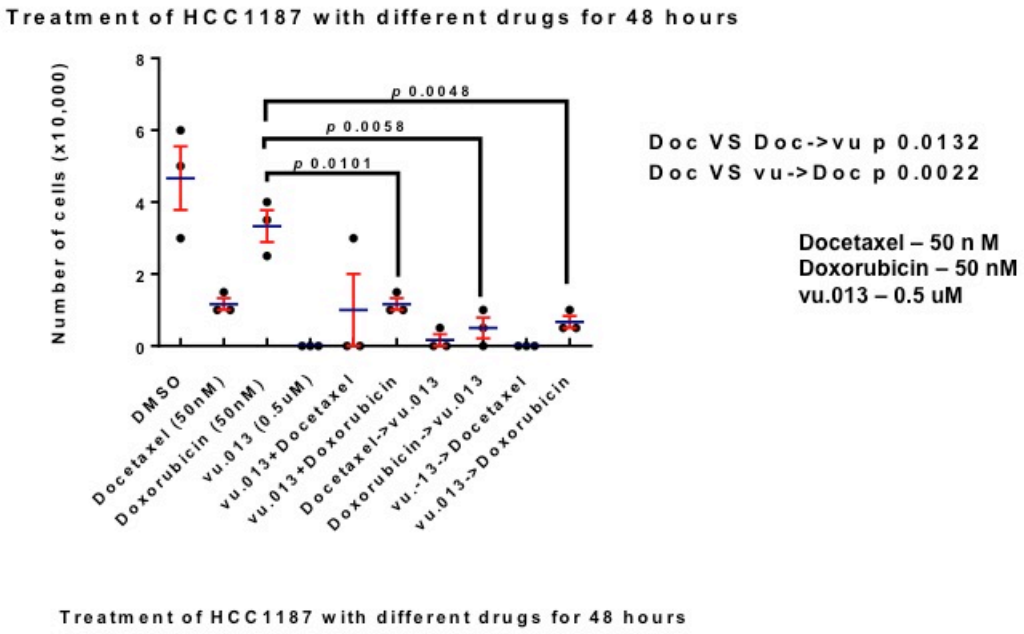

Figure S4: Quantification of the cells after treatment with different drugs for 48 hrs. 50,000 cells are plated and seeded overnight, and confirmed that cells are attached before treatment. The cells are counted manually every 48 hrs. Again, HCC-1187 cells are very sensitive to VU-013/**42**. Treatment with **42**, or combination treatment with **42**+docetaxol and **42**+doxorubicin resulted in reduced number of cells.

S5. Screening of compounds 35-43 in Mcl-1 sensitive cell line panel

Table S5: Growth Inhibition Assays in Multiple Tumor Cell Lines

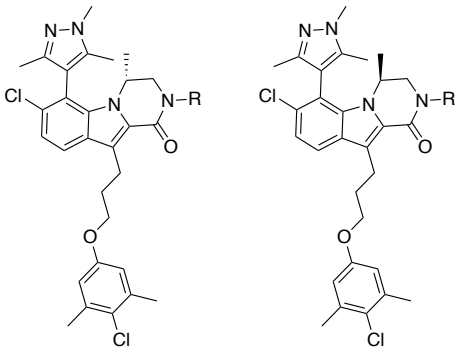

35-43 **44**

Comp.	R	GI_{50} (μM)					
		H929	AMO-1	MV-411	HCC1187	BT-20	H1703
35	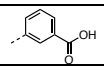	4.4±0.01	3.3±0.01	2.3±0.2	>12.5	12±1	6.9±0.5
36	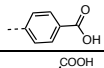	4.0±0.1	2.5±0.4	2.4±0.01	>12.5	11±2	4.7±0.6
37	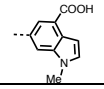	0.82±0.01	0.55±0.09	0.37±0.1	5.5±0.6	7.0±0.9	4.1±0.2
38	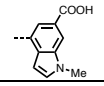	2.1±0.2	7.1±7	1.0±0.07	>12.5	9.4±4	11±0.2
39	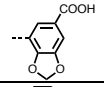	1.7±0.1	1.4±0.05	0.58±0.06	7.3±0.1	7.7±2	6.4±0.3
40	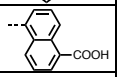	0.65±0.1	0.36±0.07	0.27±0.03	5.2±0.4	4.3±0.5	2.8±0.2
41	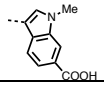	0.29±0.07	0.22±0.07	0.12±0.02	2.7±0.2	3.3±0.3	2.0±0.1
42	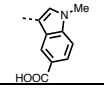	0.19±0.03	0.14±0.03	0.067±0.004	1.3±0.04	2.1±0.6	1.1±0.1
***P*-42**	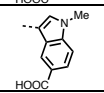	0.12±0.01	0.10±0.02	0.088±0.001	0.92±0.03	1.8±0.7	0.83±0.08
***M*-42**	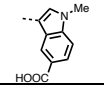	0.12±0.02	0.097±0.02	0.075±0.01	0.88±0.04	1.6±0.4	0.72±0.02
43	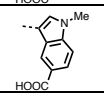	3.6±0.1	2.3±0.1	1.8±0.08	>12.5	>12.5	>12.5

S6. Synthesis and Characterization of Compounds

Compounds 1-5: Synthesis and characterization as described in Shaw et al., *J. Med. Chem.*, **2018**, *61 (6)*, pp. 2410-2421 (Ref 39).

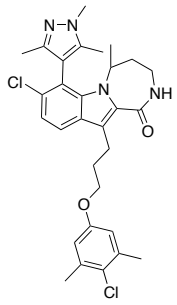

8-chloro-11-(3-(4-chloro-3,5-dimethylphenoxy)propyl)-5-methyl-7-(1,3,5-trimethyl-1H-pyrazol-4-yl)-2,3,4,5-tetrahydro-1H-[1,4]diazepino[1,2-a]indol-1-one (6):

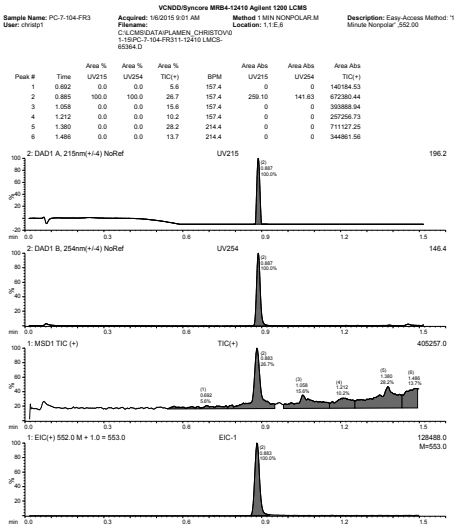

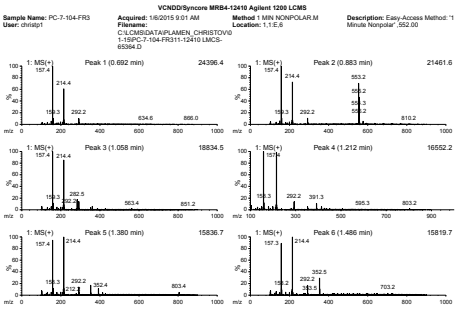

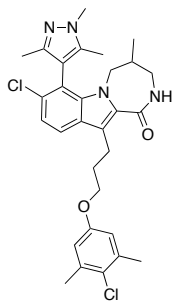

8-chloro-11-(3-(4-chloro-3,5-dimethylphenoxy)propyl)-4-methyl-7-(1,3,5-trimethyl-1H-pyrazol-4-yl)-2,3,4,5-tetrahydro-1H-[1,4]diazepino[1,2-a]indol-1-one (7):

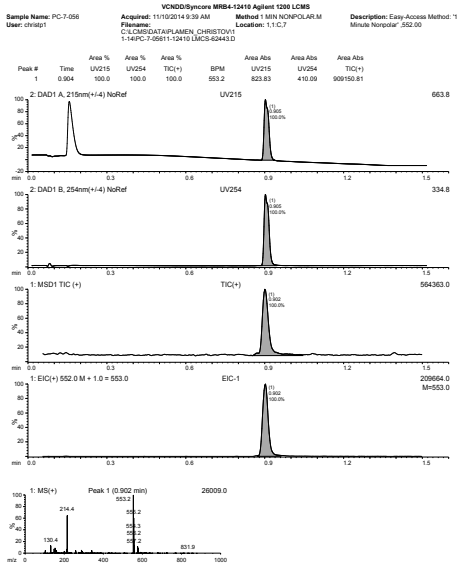

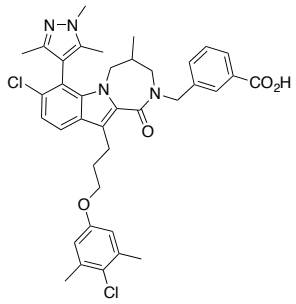

3-((8-chloro-11-(3-(4-chloro-3,5-dimethylphenoxy)propyl)-4-methyl-1-oxo-7-(1,3,5-trimethyl-1H-pyrazol-4-yl)-4,5-dihydro-1H-[1,4]diazepino[1,2-a]indol-2(3H)-yl)methyl)benzoic acid (8):

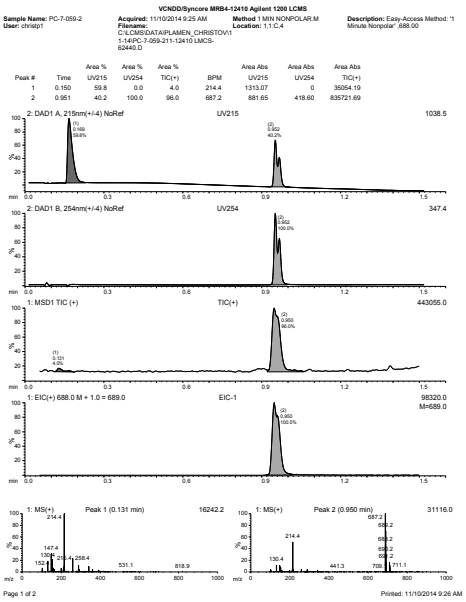

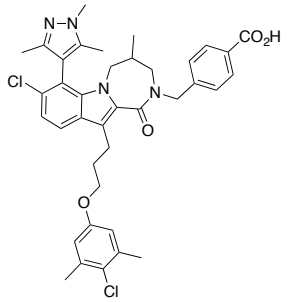

4-((8-chloro-11-(3-(4-chloro-3,5-dimethylphenoxy)propyl)-4-methyl-1-oxo-7-(1,3,5-trimethyl-1H-pyrazol-4-yl)-4,5-dihydro-1H-[1,4]diazepino[1,2-a]indol-2(3H)-yl)methyl)benzoic acid (9):

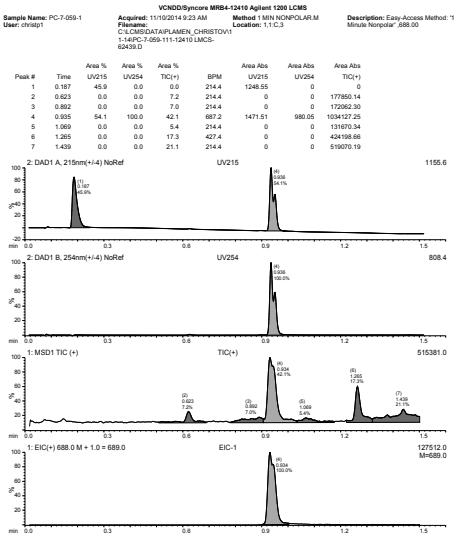

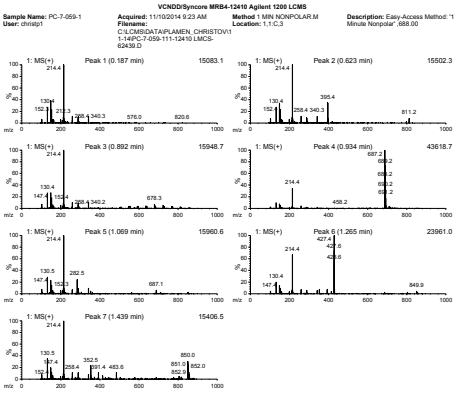

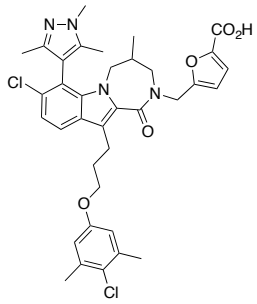

5-((8-chloro-11-(3-(4-chloro-3,5-dimethylphenoxy)propyl)-4-methyl-1-oxo-7-(1,3,5-trimethyl-1H-pyrazol-4-yl)-4,5-dihydro-1H-[1,4]diazepino[1,2-a]indol-2(3H)-yl)methyl)furan-2-carboxylic acid (10):

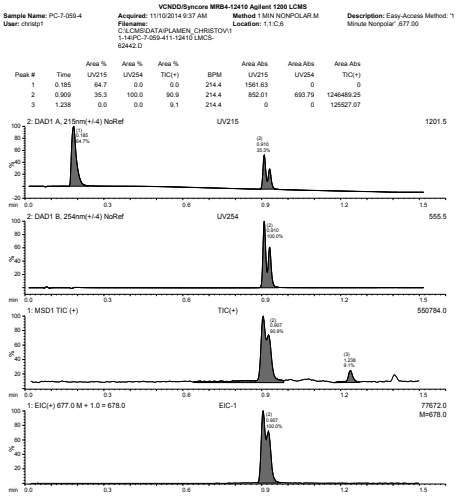

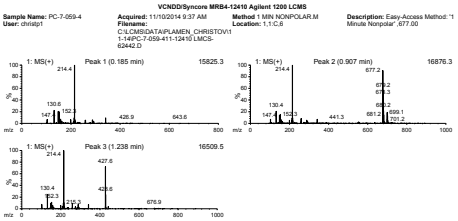

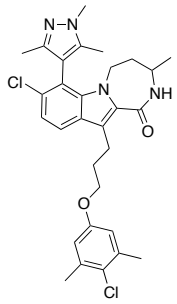

8-chloro-11-(3-(4-chloro-3,5-dimethylphenoxy)propyl)-3-methyl-7-(1,3,5-trimethyl-1H-pyrazol-4-yl)-2,3,4,5-tetrahydro-1H-[1,4]diazepino[1,2-a]indol-1-one (11):

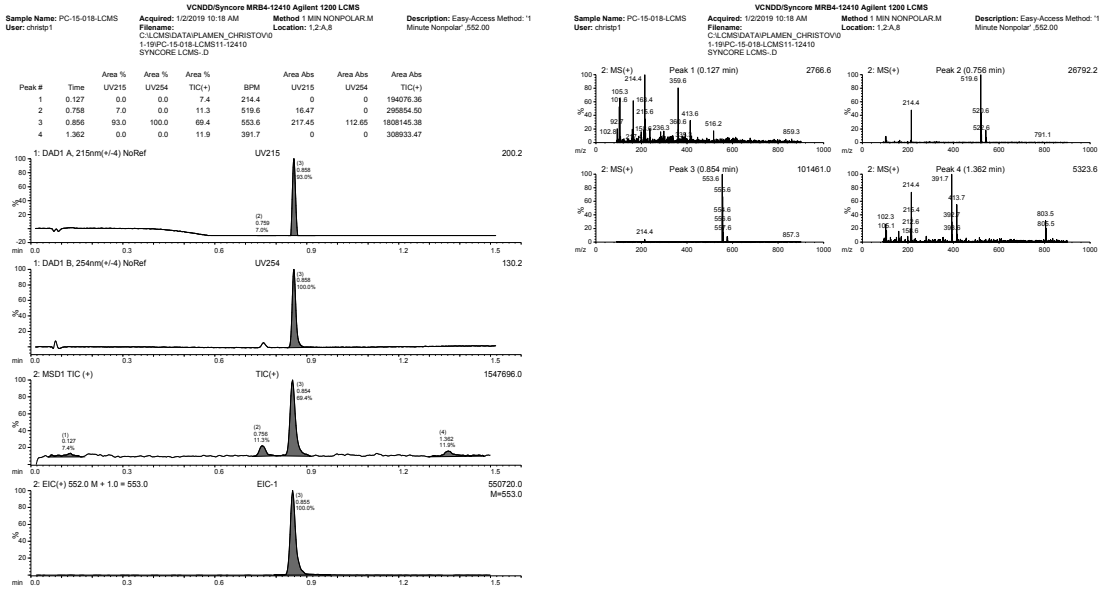

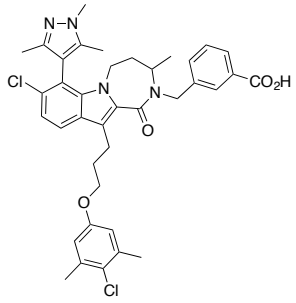

3-((8-chloro-11-(3-(4-chloro-3,5-dimethylphenoxy)propyl)-3-methyl-1-oxo-7-(1,3,5-trimethyl-1H-pyrazol-4-yl)-4,5-dihydro-1H-[1,4]diazepino[1,2-a]indol-2(3H)-yl)methyl)benzoic acid (12):

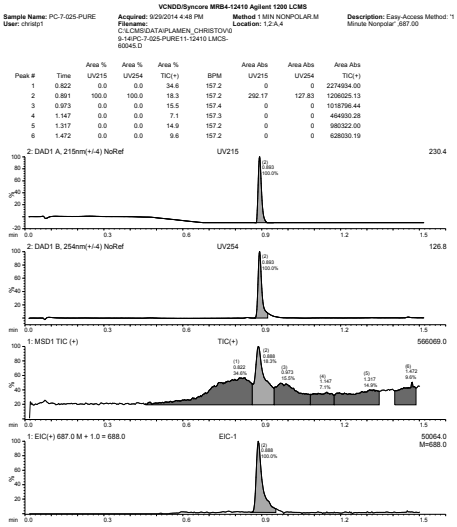

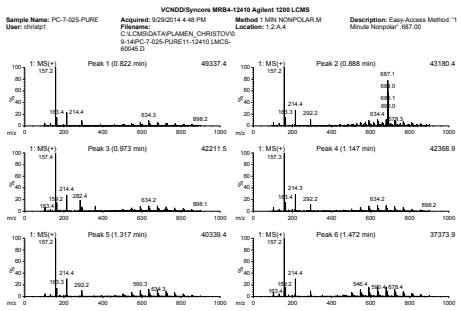

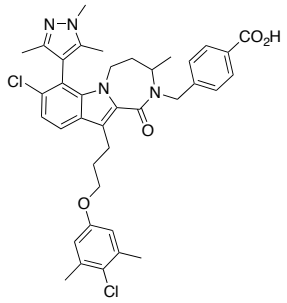

4-((8-chloro-11-(3-(4-chloro-3,5-dimethylphenoxy)propyl)-3-methyl-1-oxo-7-(1,3,5-trimethyl-1H-pyrazol-4-yl)-4,5-dihydro-1H-[1,4]diazepino[1,2-a]indol-2(3H)-yl)methyl)benzoic acid (13):

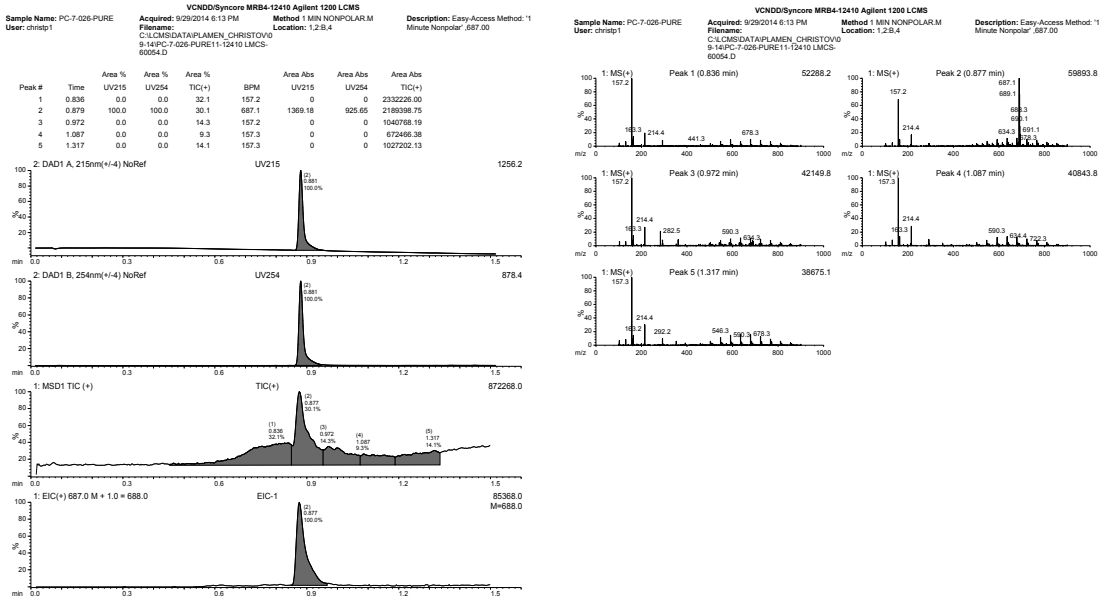

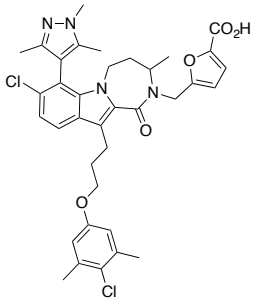

5-((8-chloro-11-(3-(4-chloro-3,5-dimethylphenoxy)propyl)-3-methyl-1-oxo-7-(1,3,5-trimethyl-1H-pyrazol-4-yl)-4,5-dihydro-1H-[1,4]diazepino[1,2-a]indol-2(3H)-yl)methyl)furan-2-carboxylic acid (14):

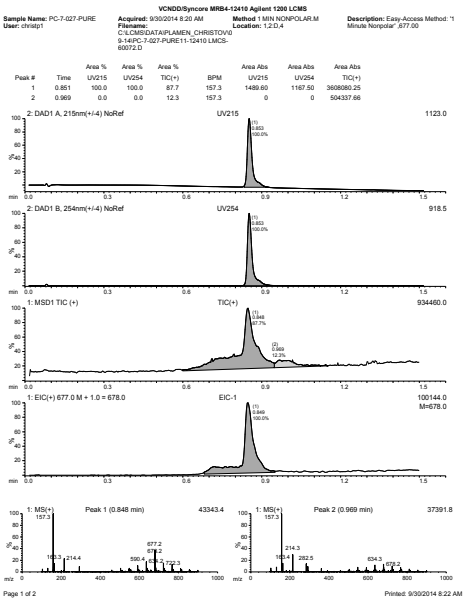

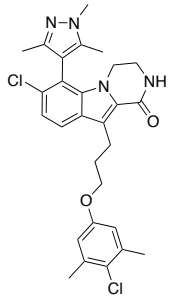

7-chloro-10-(3-(4-chloro-3,5-dimethylphenoxy)propyl)-6-(1,3,5-trimethyl-1H-pyrazol-4-yl)-3,4-dihydropyrazino[1,2-a]indol-1(2H)-one (15):

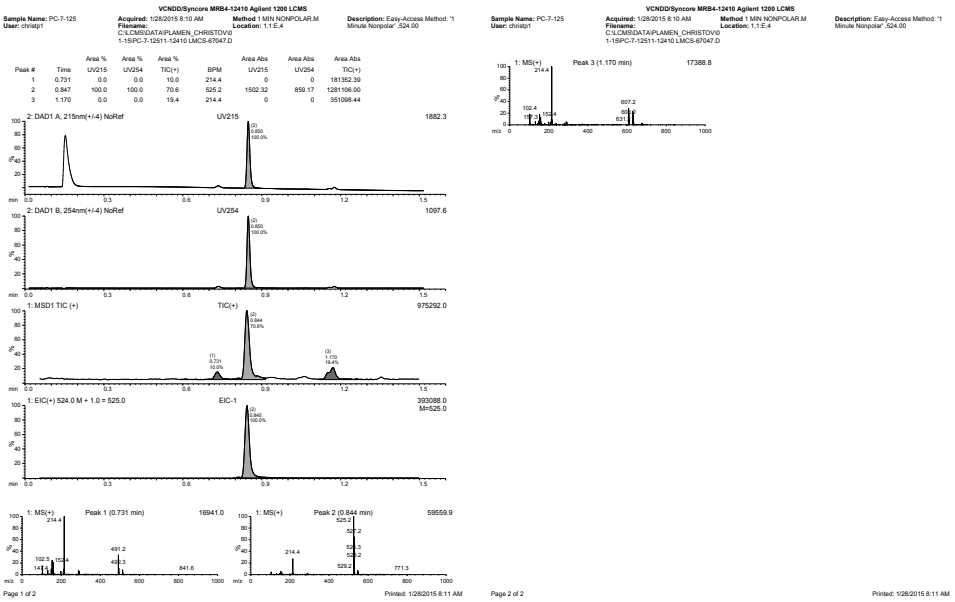

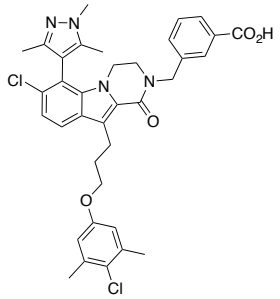

3-((7-chloro-10-(3-(4-chloro-3,5-dimethylphenoxy)propyl)-1-oxo-6-(1,3,5-trimethyl-1H-pyrazol-4-yl)-3,4-dihydropyrazino[1,2-a]indol-2(1H)-yl)methyl)benzoic acid (16):

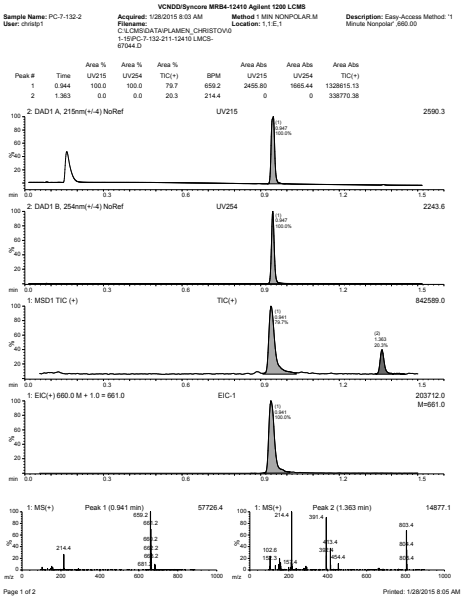

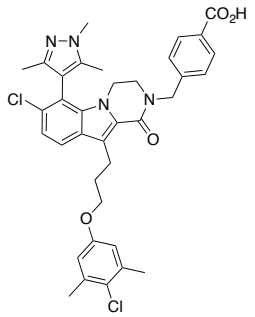

4-((7-chloro-10-(3-(4-chloro-3,5-dimethylphenoxy)propyl)-1-oxo-6-(1,3,5-trimethyl-1H-pyrazol-4-yl)-3,4-dihydropyrazino[1,2-a]indol-2(1H)-yl)methyl)benzoic acid (17):

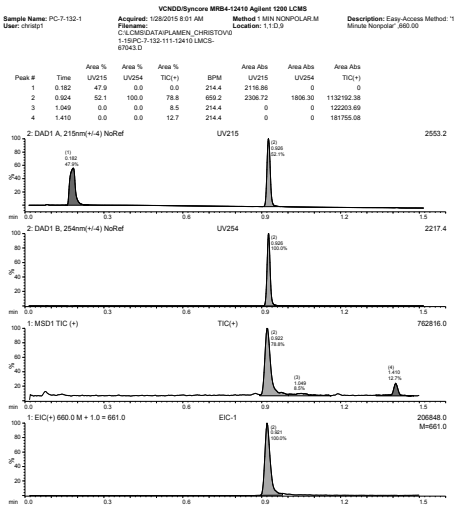

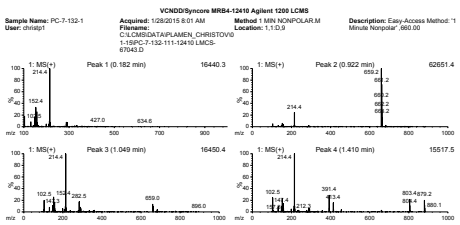

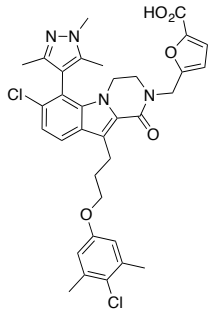

5-((7-chloro-10-(3-(4-chloro-3,5-dimethylphenoxy)propyl)-1-oxo-6-(1,3,5-trimethyl-1H-pyrazol-4-yl)-3,4-dihydropyrazino[1,2-a]indol-2(1H)-yl)methyl)furan-2-carboxylic acid (18):

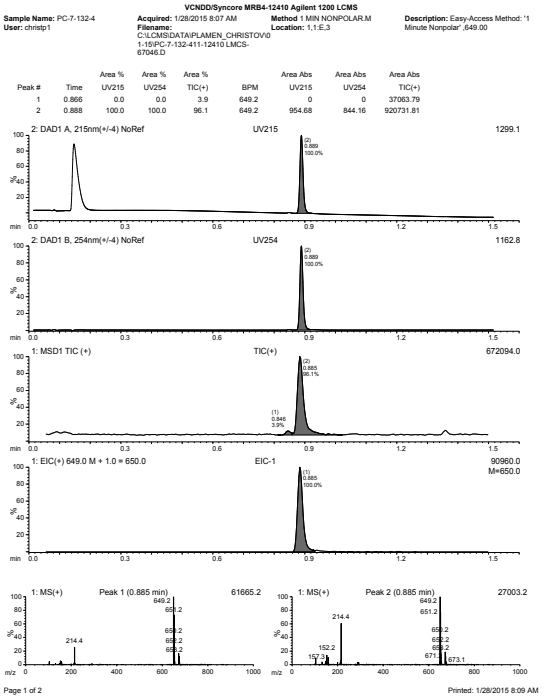

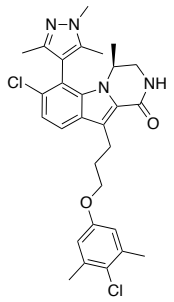

(*S*)-7-chloro-10-(3-(4-chloro-3,5-dimethylphenoxy)propyl)-4-methyl-6-(1,3,5-trimethyl-1H-pyrazol-4-yl)-3,4-dihydropyrazino[1,2-a]indol-1(2H)-one (19):

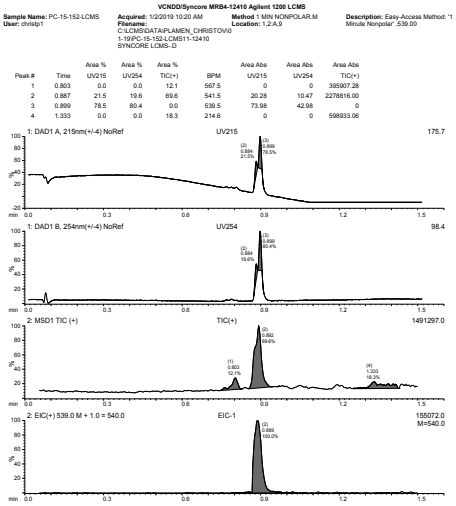

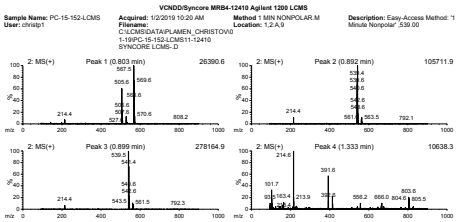

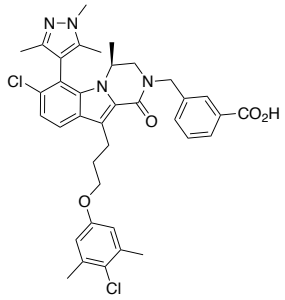

(*S*)-3-((7-chloro-10-(3-(4-chloro-3,5-dimethylphenoxy)propyl)-4-methyl-1-oxo-6-(1,3,5-trimethyl-1H-pyrazol-4-yl)-3,4-dihydropyrazino[1,2-a]indol-2(1H)-yl)methyl)benzoic acid (20):

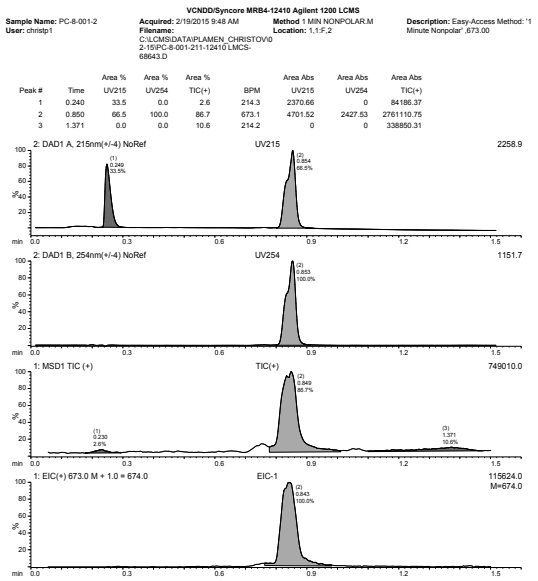

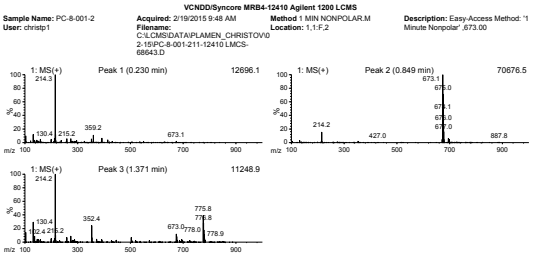

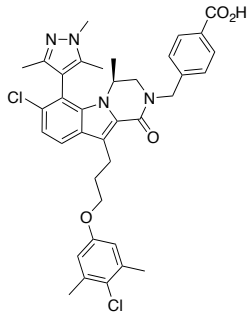

(*S*)-4-((7-chloro-10-(3-(4-chloro-3,5-dimethylphenoxy)propyl)-4-methyl-1-oxo-6-(1,3,5-trimethyl-1H-pyrazol-4-yl)-3,4-dihydropyrazino[1,2-a]indol-2(1H)-yl)methyl)benzoic acid (21):

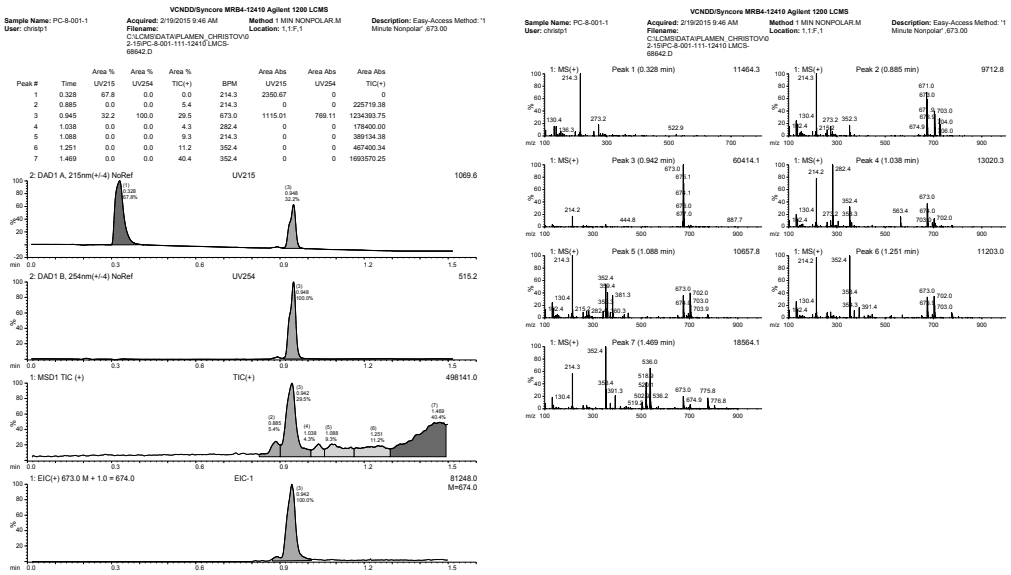

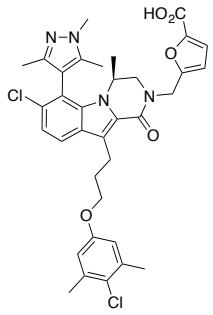

(*S*)-5-((7-chloro-10-(3-(4-chloro-3,5-dimethylphenoxy)propyl)-4-methyl-1-oxo-6-(1,3,5-trimethyl-1H-pyrazol-4-yl)-3,4-dihydropyrazino[1,2-a]indol-2(1H)-yl)methyl)furan-2-carboxylic acid (22):

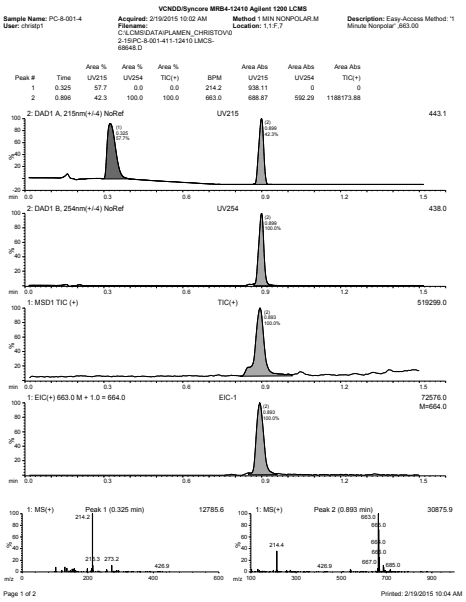

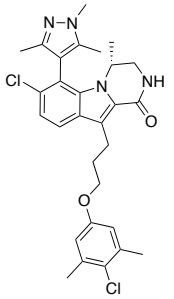

(*R*)-7-chloro-10-(3-(4-chloro-3,5-dimethylphenoxy)propyl)-4-methyl-6-(1,3,5-trimethyl-1H-pyrazol-4-yl)-3,4-dihydropyrazino[1,2-a]indol-1(2H)-one (23):

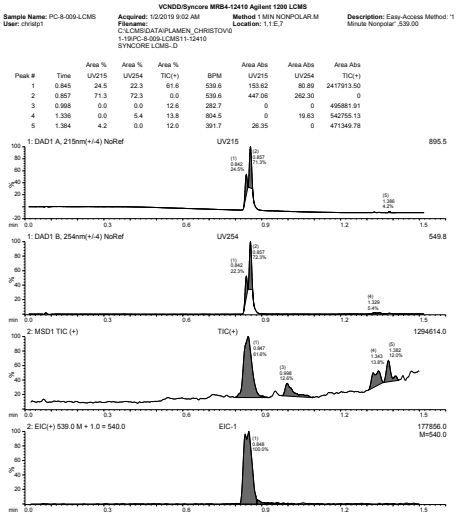

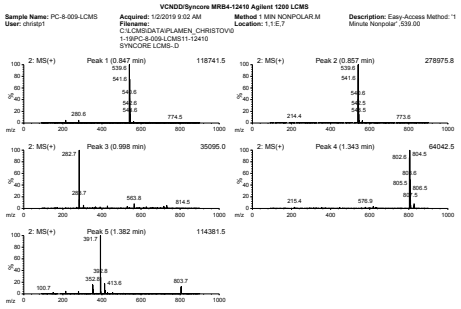

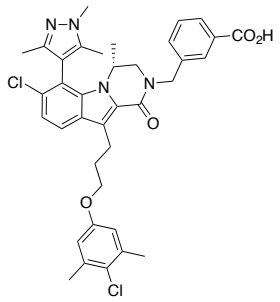

(*R*)-3-((7-chloro-10-(3-(4-chloro-3,5-dimethylphenoxy)propyl)-4-methyl-1-oxo-6-(1,3,5-trimethyl-1H-pyrazol-4-yl)-3,4-dihydropyrazino[1,2-a]indol-2(1H)-yl)methyl)benzoic acid (24):

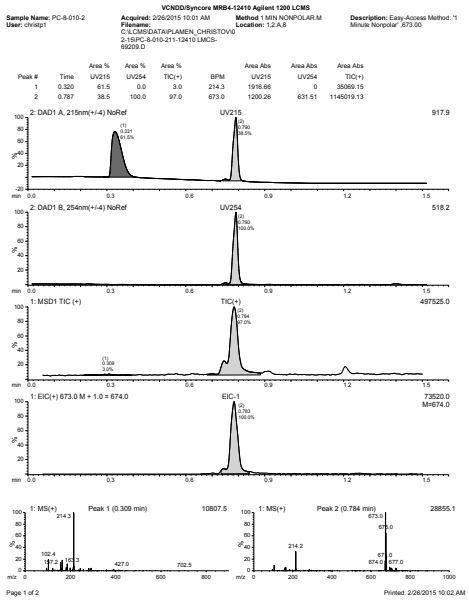

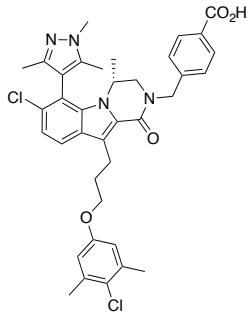

(*R*)-4-((7-chloro-10-(3-(4-chloro-3,5-dimethylphenoxy)propyl)-4-methyl-1-oxo-6-(1,3,5-trimethyl-1H-pyrazol-4-yl)-3,4-dihydropyrazino[1,2-a]indol-2(1H)-yl)methyl)benzoic acid (25):

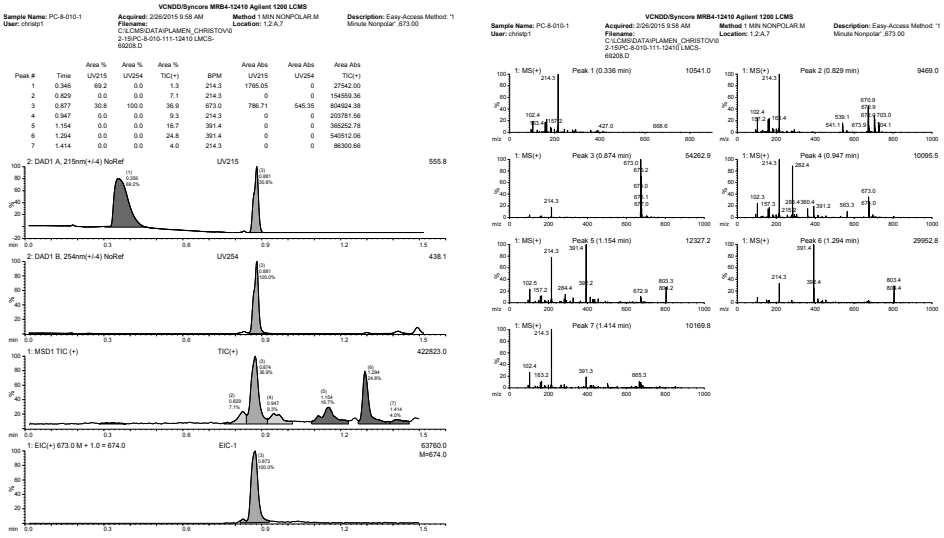

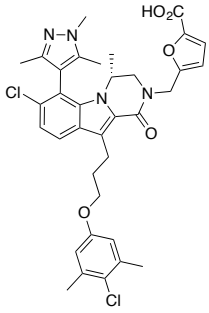

(*R*)-5-((7-chloro-10-(3-(4-chloro-3,5-dimethylphenoxy)propyl)-4-methyl-1-oxo-6-(1,3,5-trimethyl-1H-pyrazol-4-yl)-3,4-dihydropyrazino[1,2-a]indol-2(1H)-yl)methyl)furan-2-carboxylic acid (26):

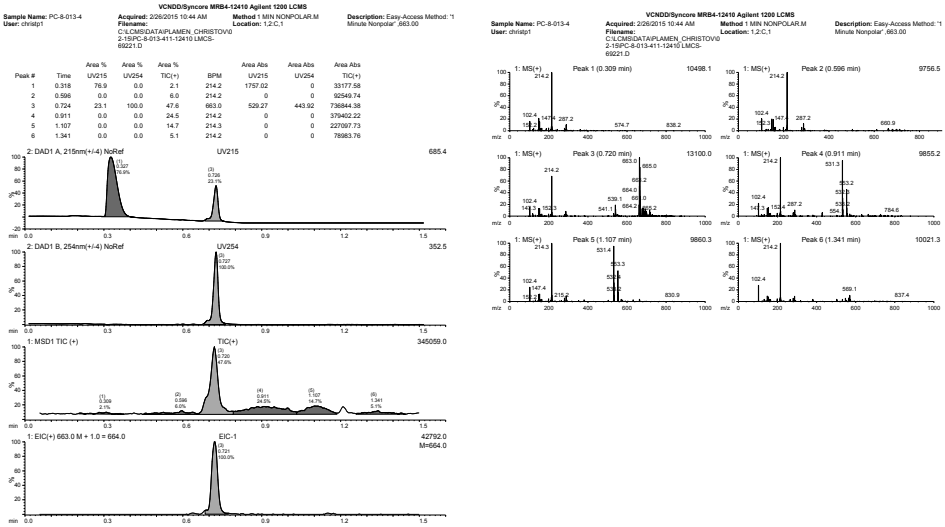

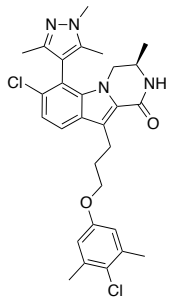

(*R*)-7-chloro-10-(3-(4-chloro-3,5-dimethylphenoxy)propyl)-3-methyl-6-(1,3,5-trimethyl-1H-pyrazol-4-yl)-3,4-dihydropyrazino[1,2-a]indol-1(2H)-one (27):

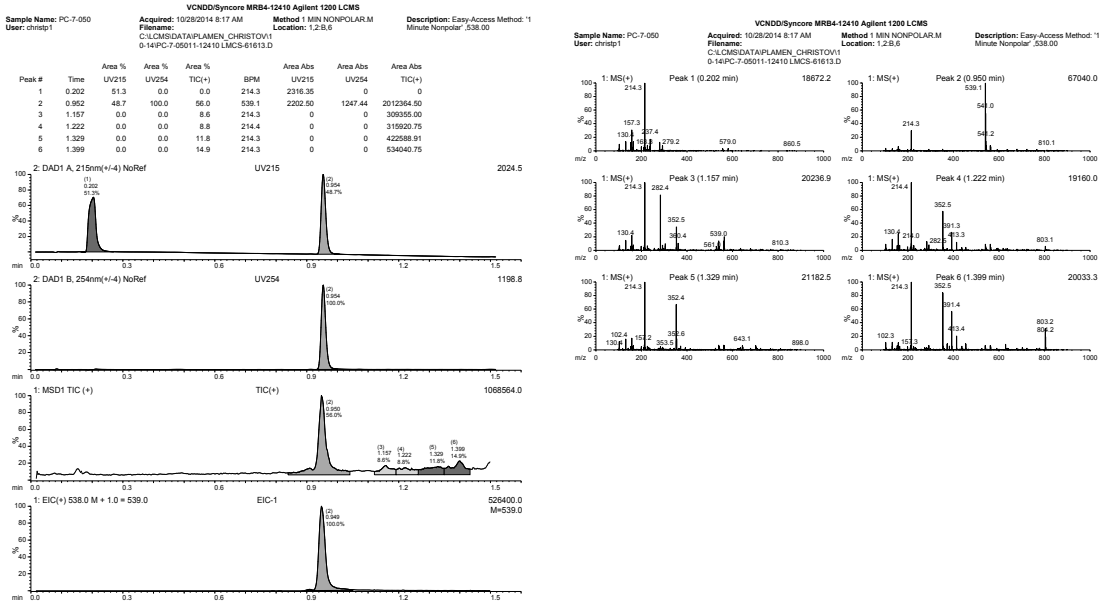

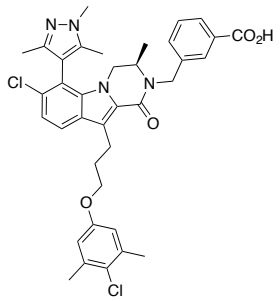

(*R*)-3-((7-chloro-10-(3-(4-chloro-3,5-dimethylphenoxy)propyl)-3-methyl-1-oxo-6-(1,3,5-trimethyl-1H-pyrazol-4-yl)-3,4-dihydropyrazino[1,2-a]indol-2(1H)-yl)methyl)benzoic acid (28):

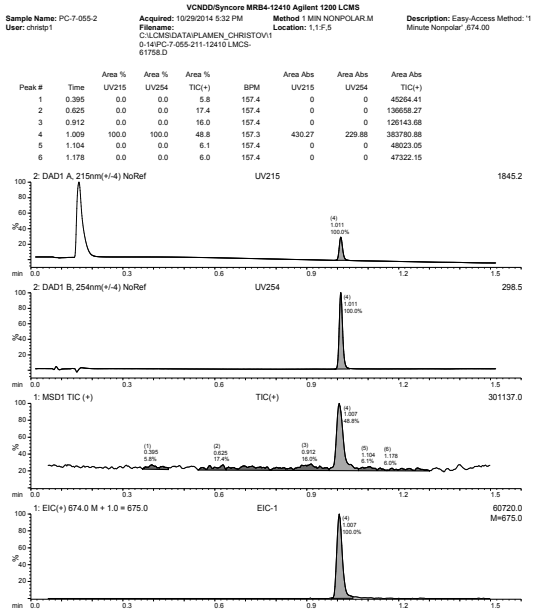

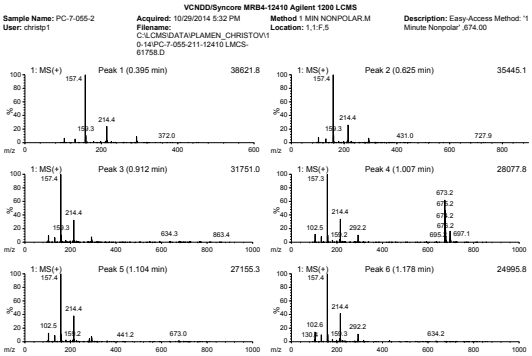

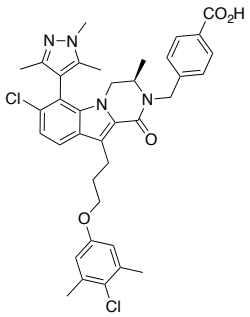

(*R*)-4-((7-chloro-10-(3-(4-chloro-3,5-dimethylphenoxy)propyl)-3-methyl-1-oxo-6-(1,3,5-trimethyl-1H-pyrazol-4-yl)-3,4-dihydropyrazino[1,2-a]indol-2(1H)-yl)methyl)benzoic acid (29):

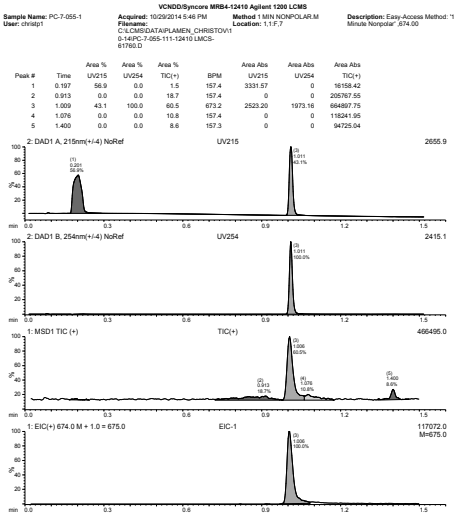

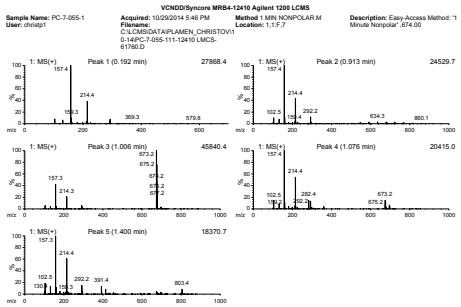

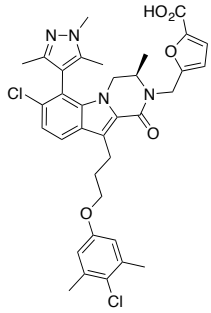

(*R*)-5-((7-chloro-10-(3-(4-chloro-3,5-dimethylphenoxy)propyl)-3-methyl-1-oxo-6-(1,3,5-trimethyl-1H-pyrazol-4-yl)-3,4-dihydropyrazino[1,2-a]indol-2(1H)-yl)methyl)furan-2-carboxylic acid (30):

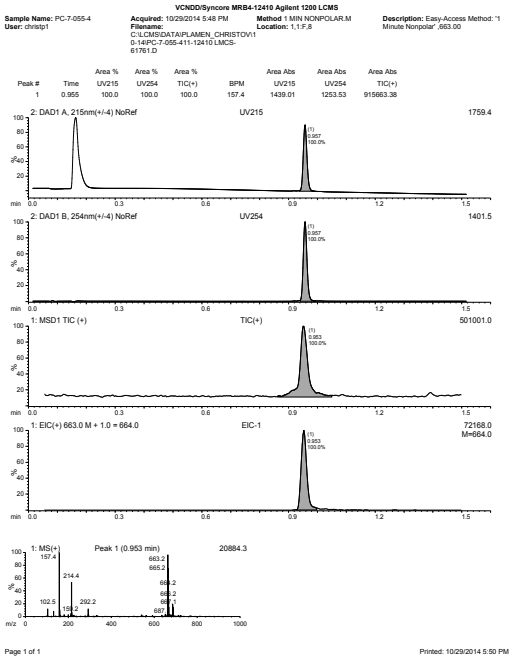

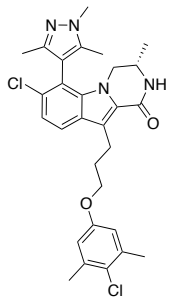

(*S*)-7-chloro-10-(3-(4-chloro-3,5-dimethylphenoxy)propyl)-3-methyl-6-(1,3,5-trimethyl-1H-pyrazol-4-yl)-3,4-dihydropyrazino[1,2-a]indol-1(2H)-one (31):

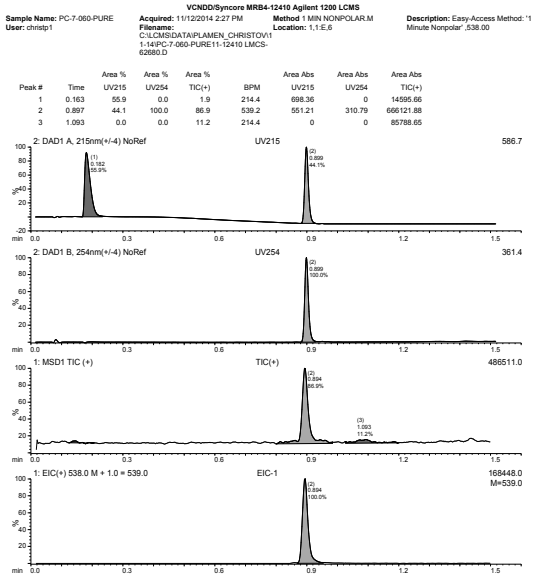

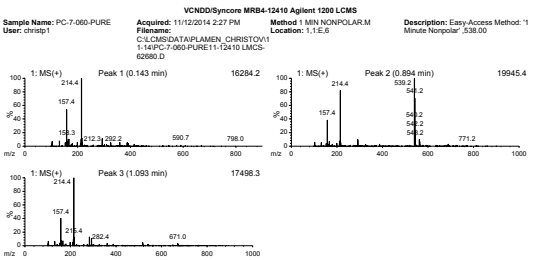

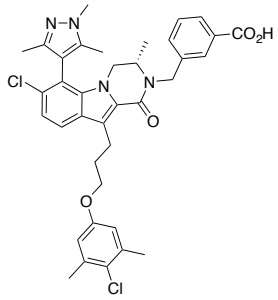

(*S*)-3-((7-chloro-10-(3-(4-chloro-3,5-dimethylphenoxy)propyl)-3-methyl-1-oxo-6-(1,3,5-trimethyl-1H-pyrazol-4-yl)-3,4-dihydropyrazino[1,2-a]indol-2(1H)-yl)methyl)benzoic acid (32):

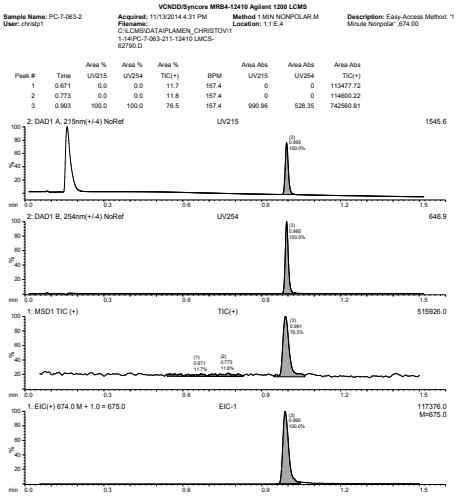

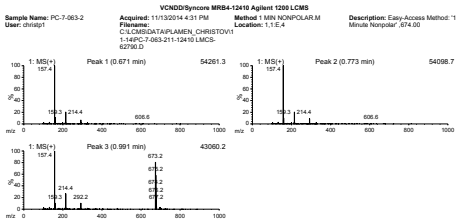

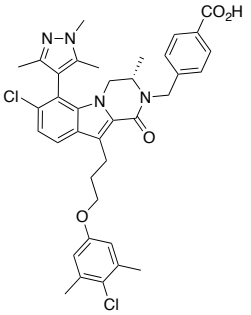

(*S*)-4-((7-chloro-10-(3-(4-chloro-3,5-dimethylphenoxy)propyl)-3-methyl-1-oxo-6-(1,3,5-trimethyl-1H-pyrazol-4-yl)-3,4-dihydropyrazino[1,2-a]indol-2(1H)-yl)methyl)benzoic acid (33):

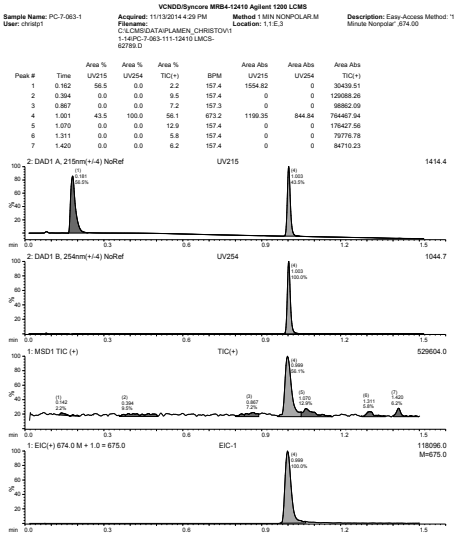

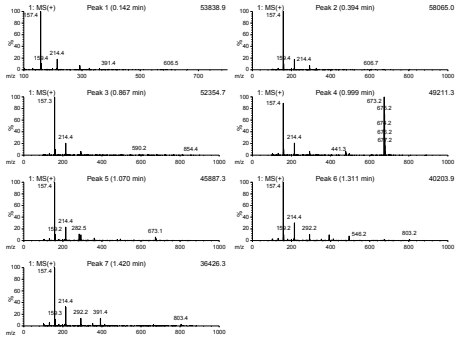

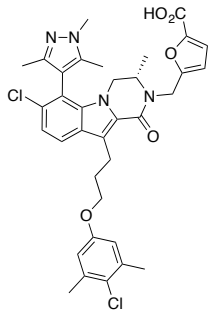

(*S*)-5-((7-chloro-10-(3-(4-chloro-3,5-dimethylphenoxy)propyl)-3-methyl-1-oxo-6-(1,3,5-trimethyl-1H-pyrazol-4-yl)-3,4-dihydropyrazino[1,2-a]indol-2(1H)-yl)methyl)furan-2-carboxylic acid (34):

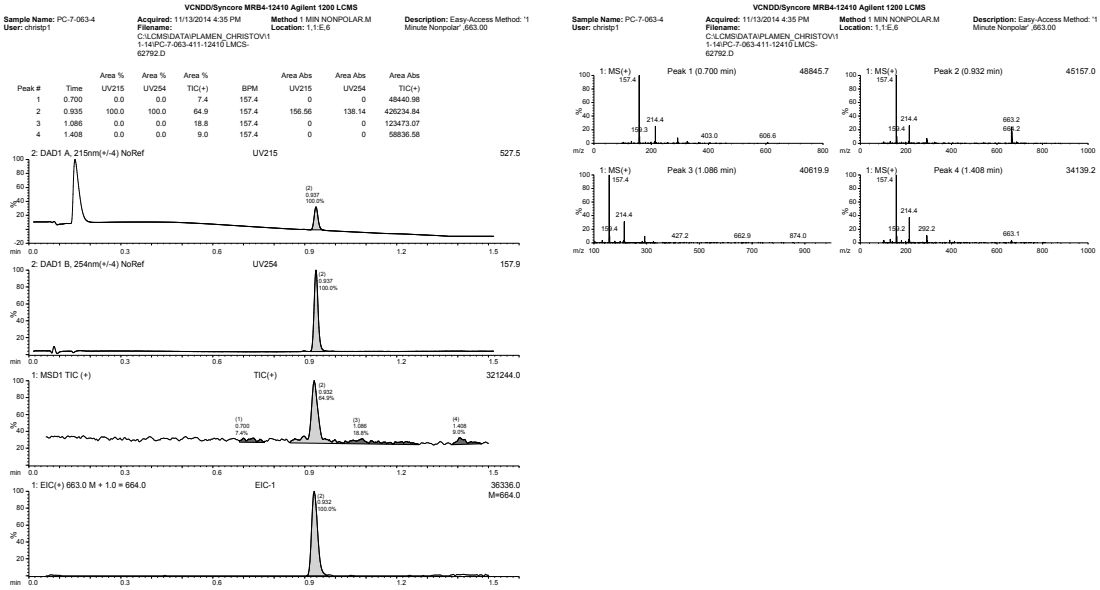

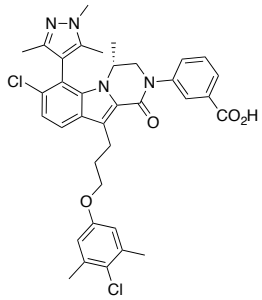

(*R*)-3-(7-chloro-10-(3-(4-chloro-3,5-dimethylphenoxy)propyl)-4-methyl-1-oxo-6-(1,3,5-trimethyl-1H-pyrazol-4-yl)-3,4-dihydropyrazino[1,2-a]indol-2(1H)-yl)benzoic acid (35):

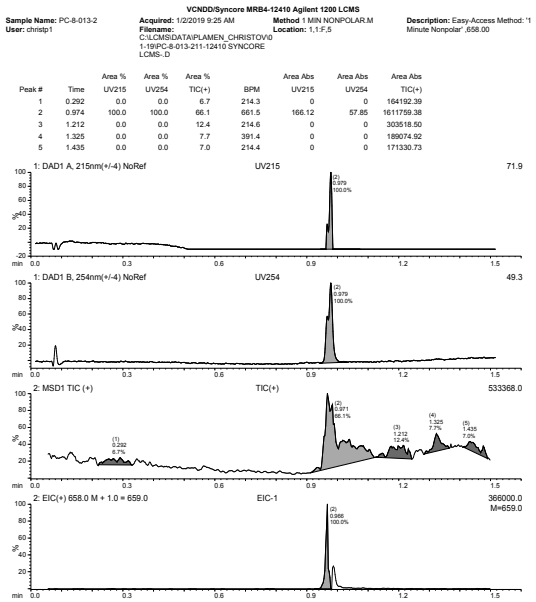

Peak #	Time	Area % UV215	Area % UV254	Area % TIC(+)	BPM	Area Abs UV215	Area Abs UV254	Area Abs TIC(+)
1	0.292	0.0	0.0	6.7	214.3	0	0	164192.39
2	0.974	100.0	100.0	66.1	661.5	166.12	57.85	1611759.38
3	1.212	0.0	0.0	12.4	214.6	0	0	303518.50
4	1.325	0.0	0.0	7.7	391.4	0	0	189074.92
5	1.435	0.0	0.0	7.0	214.4	0	0	171330.73

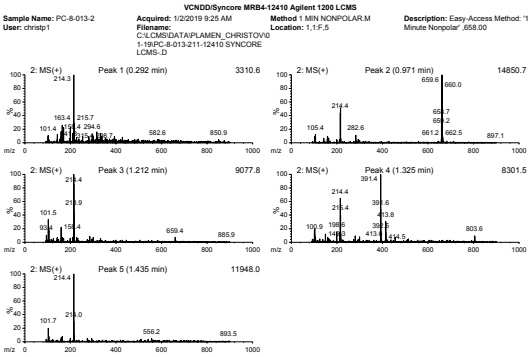

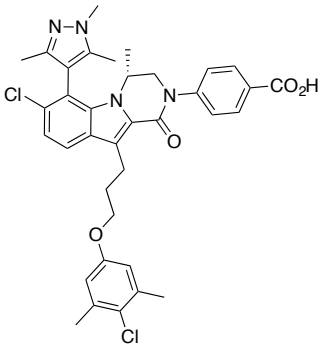

(*R*)-4-(7-chloro-10-(3-(4-chloro-3,5-dimethylphenoxy)propyl)-4-methyl-1-oxo-6-(1,3,5-trimethyl-1H-pyrazol-4-yl)-3,4-dihydropyrazino[1,2-a]indol-2(1H)-yl)benzoic acid (36):

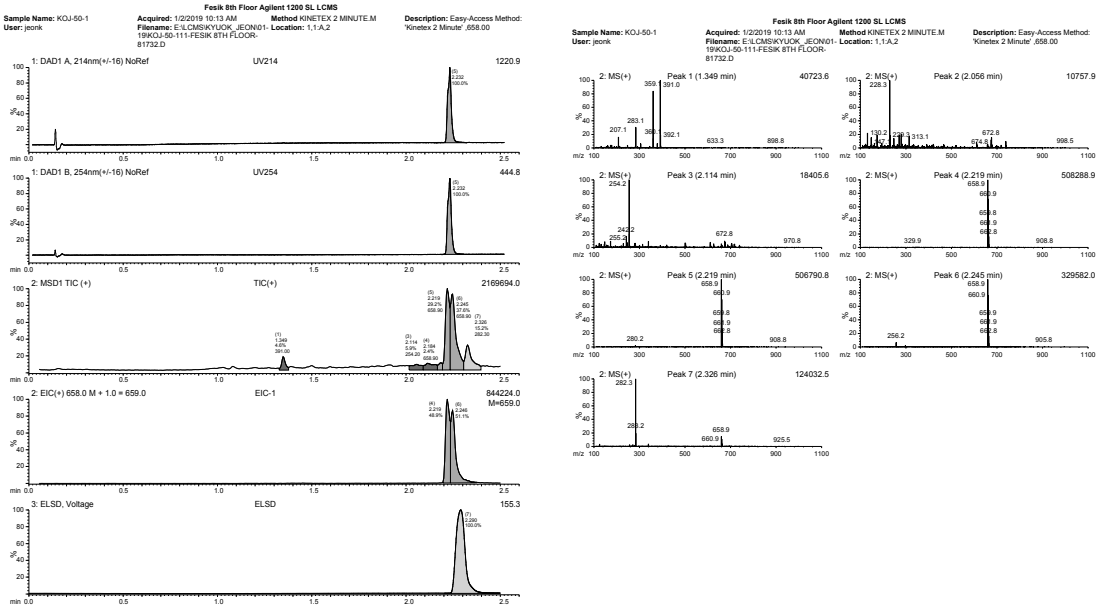

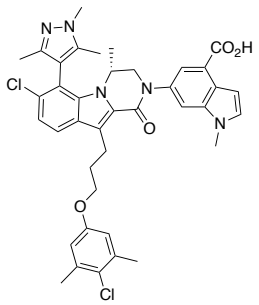

(*R*)-6-(7-chloro-10-(3-(4-chloro-3,5-dimethylphenoxy)propyl)-4-methyl-1-oxo-6-(1,3,5-trimethyl-1*H*-pyrazol-4-yl)-3,4-dihydropyrazino[1,2-*a*]indol-2(1*H*)-yl)-1-methyl-1*H*-indole-4-carboxylic acid (37):

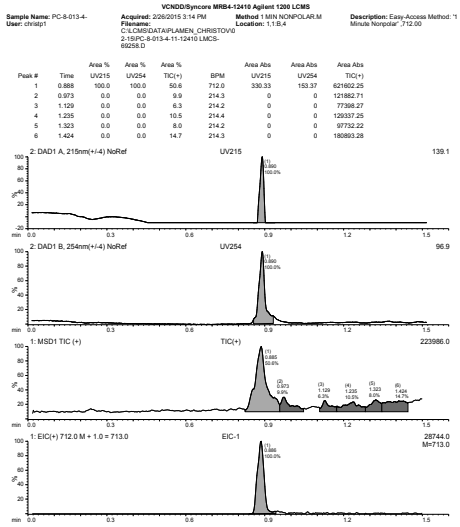

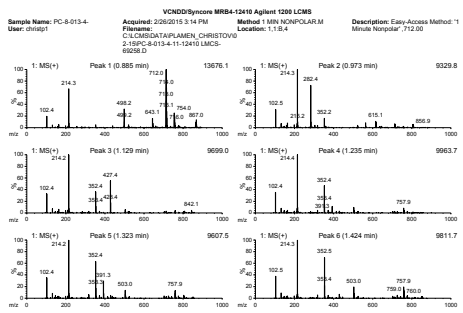

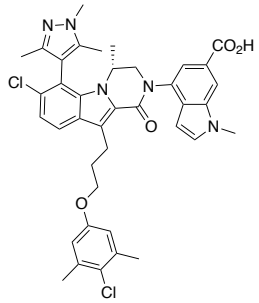

(*R*)-4-(7-chloro-10-(3-(4-chloro-3,5-dimethylphenoxy)propyl)-4-methyl-1-oxo-6-(1,3,5-trimethyl-1H-pyrazol-4-yl)-3,4-dihydropyrazino[1,2-a]indol-2(1H)-yl)-1-methyl-1H-indole-6-carboxylic acid (38):

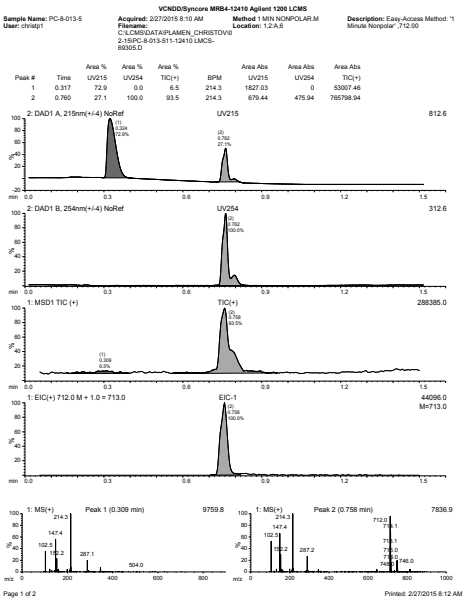

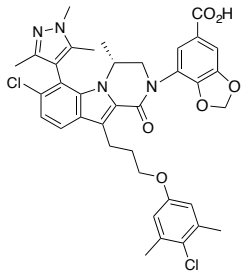

(*R*)-7-(7-chloro-10-(3-(4-chloro-3,5-dimethylphenoxy)propyl)-4-methyl-1-oxo-6-(1,3,5-trimethyl-1*H*-pyrazol-4-yl)-3,4-dihydropyrazino[1,2-*a*]indol-2(1*H*)-yl)benzo[*d*][1,3]dioxole-5-carboxylic acid (39)

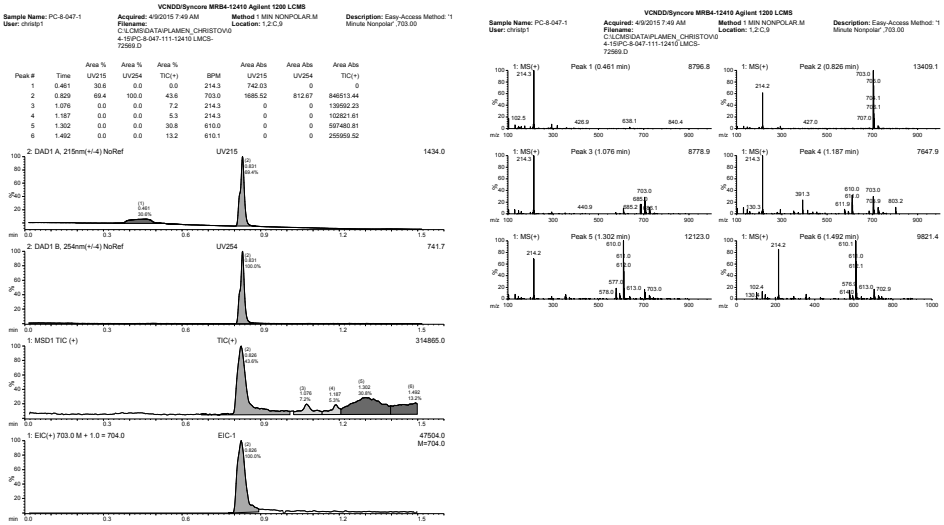

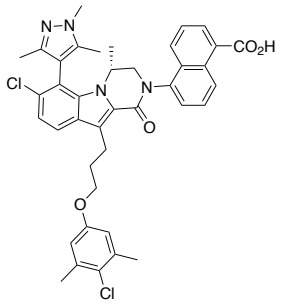

5-(7-chloro-10-(3-(4-chloro-3,5-dimethylphenoxy)propyl)-4-methyl-1-oxo-6-(1,3,5-trimethyl-1*H*-pyrazol-4-yl)-3,4-dihydropyrazino[1,2-*a*]indol-2(1*H*)-yl)-1-naphthoic acid (40):

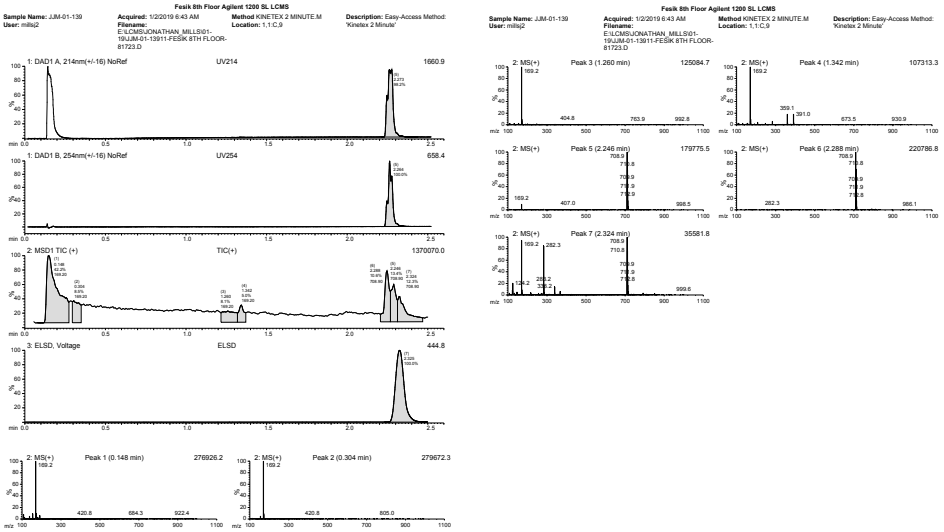

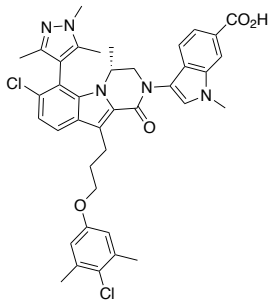

(*R*)-3-(7-chloro-10-(3-(4-chloro-3,5-dimethylphenoxy)propyl)-4-methyl-1-oxo-6-(1,3,5-trimethyl-1*H*-pyrazol-4-yl)-3,4-dihydropyrazino[1,2-*a*]indol-2(1*H*)-yl)-1-methyl-1*H*-indole-6-carboxylic acid (41):

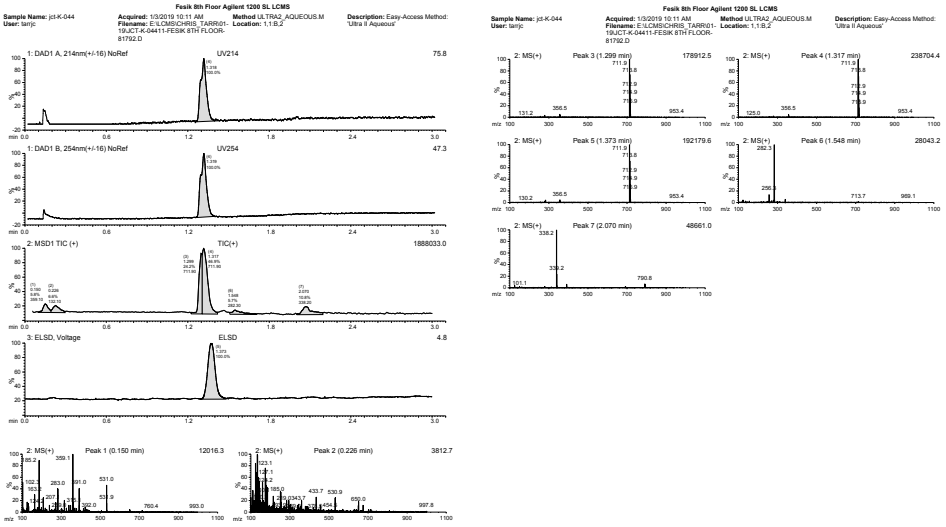

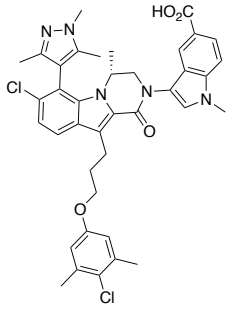

(*R*)-3-(7-chloro-10-(3-(4-chloro-3,5-dimethylphenoxy)propyl)-4-methyl-1-oxo-6-(1,3,5-trimethyl-1*H*-pyrazol-4-yl)-3,4-dihydropyrazino[1,2-*a*]indol-2(1*H*)-yl)-1-methyl-1*H*-indole-5-carboxylic acid (42):

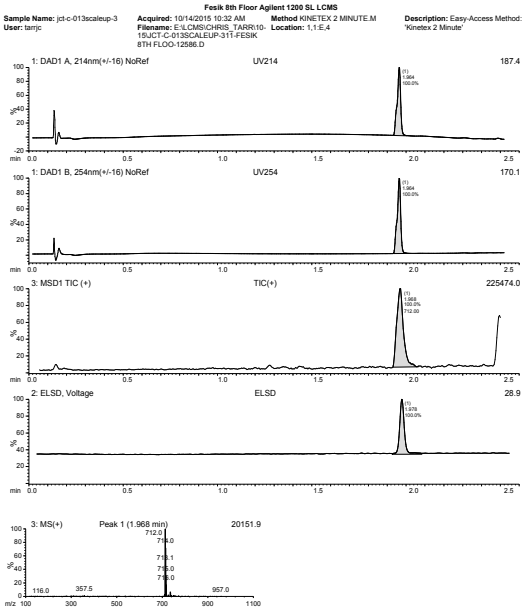

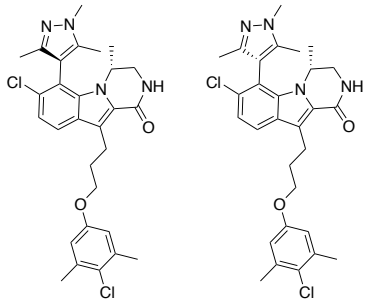

Separation of lactam atropisomers:

(*M*)-(*R*)-7-chloro-10-(3-(4-chloro-3,5-dimethylphenoxy)propyl)-4-methyl-6-(1,3,5-trimethyl-1*H*-pyrazol-4-yl)-3,4-dihydropyrazino[1,2-*a*]indol-1(2*H*)-one (second eluting atropisomer)

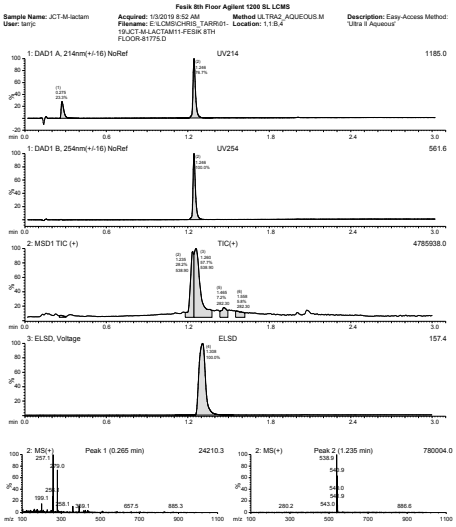

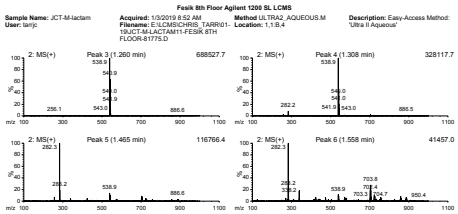

(*P*)-(*R*)-7-chloro-10-(3-(4-chloro-3,5-dimethylphenoxy)propyl)-4-methyl-6-(1,3,5-trimethyl-1*H*-pyrazol-4-yl)-3,4-dihydropyrazino[1,2-*a*]indol-1(2*H*)-one (first eluting atropisomer)

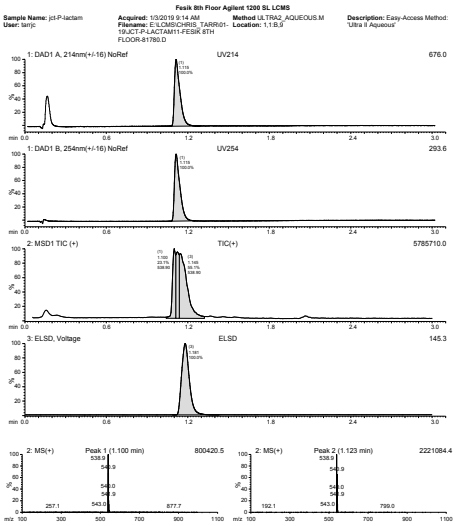

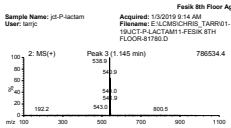

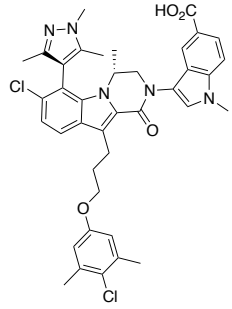

(*M*)-(*R*)-3-(7-chloro-10-(3-(4-chloro-3,5-dimethylphenoxy)propyl)-4-methyl-1-oxo-6-(1,3,5-trimethyl-1*H*-pyrazol-4-yl)-3,4-dihydropyrazino[1,2-*a*]indol-2(1*H*)-yl)-1-methyl-1*H*-indole-5-carboxylic acid ((*M*)-42):

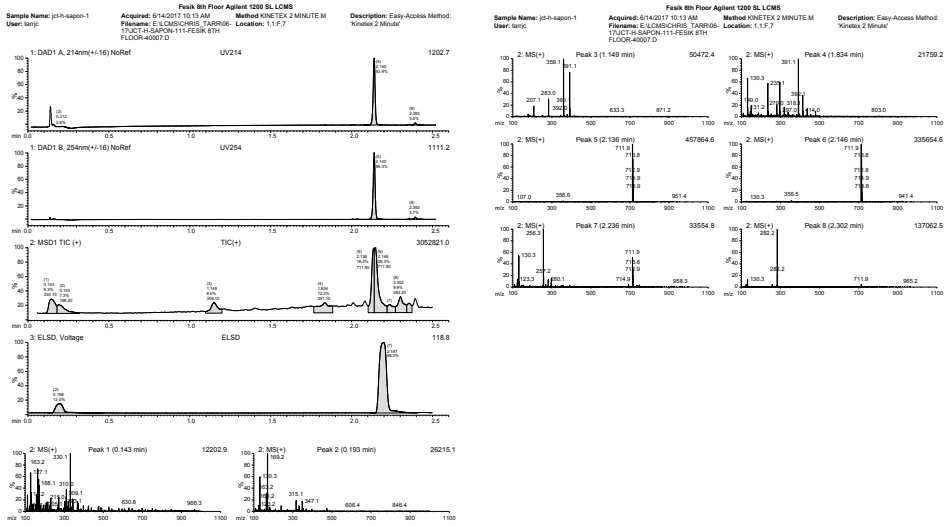

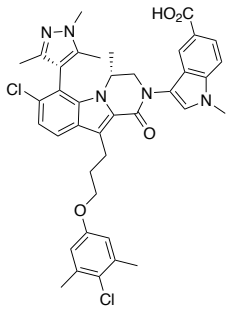

(*P*)-(*R*)-3-(7-chloro-10-(3-(4-chloro-3,5-dimethylphenoxy)propyl)-4-methyl-1-oxo-6-(1,3,5-trimethyl-1*H*-pyrazol-4-yl)-3,4-dihydropyrazino[1,2-*a*]indol-2(1*H*)-yl)-1-methyl-1*H*-indole-5-carboxylic acid ((*P*)-42):

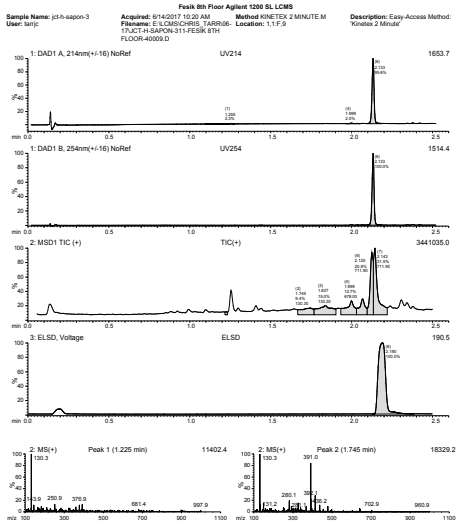

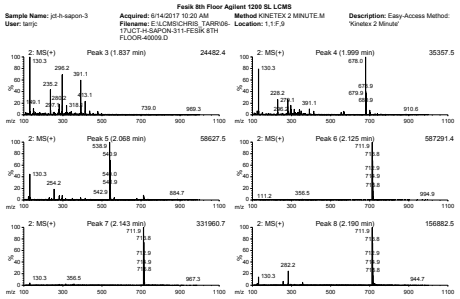

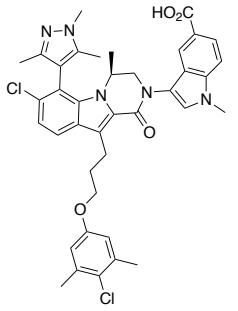

(*S*)-3-(7-chloro-10-(3-(4-chloro-3,5-dimethylphenoxy)propyl)-4-methyl-1-oxo-6-(1,3,5-trimethyl-1*H*-pyrazol-4-yl)-3,4-dihydropyrazino[1,2-*a*]indol-2(1*H*)-yl)-1-methyl-1*H*-indole-5-carboxylic acid (43):

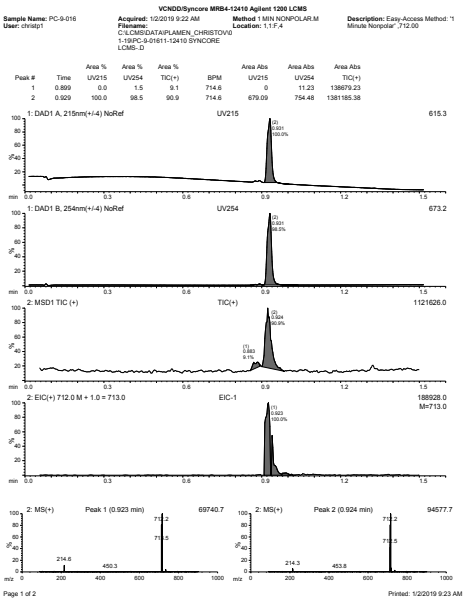
VCNDD/Syncore MRB4-12410 Agilent 1200 LCMS
Sample Name: PC-9-016
User: christp1
Acquired: 1/2/2019 9:22 AM
Filename: C:\LCMSDATA\PLAMEN_CHRISTOV\0 1-19\PC-9-016\1-12410 SYNCORE LCMS-.D
Method 1 MIN NONPOLAR.M
Location: 1.1.F.4
Description: Easy-Access Method: "1 Minute Nonpolar" ,712.00
Peak # Time Area % UV215 Area % UV254 Area % TIC(+) BPM Area Abs UV215 Area Abs UV254 Area Abs TIC(+)
1 0.899 0.0 1.5 9.1 714.6 0 11.23 138679.23
2 0.929 100.0 98.5 90.9 714.6 679.09 754.48 1381185.38
1: DAD1 A, 215nm(+/-4) NoRef
UV215
615.3
1: DAD1 B, 254nm(+/-4) NoRef
UV254
673.2
2: MSD1 TIC (+)
TIC(+)
1121626.0
2: EIC(+) 712.0 M + 1.0 = 713.0
EIC-1
188928.0
M=713.0
2: MS(+)
Peak 1 (0.923 min)
69740.7
214.6
450.3
712.2
713.5
2: MS(+)
Peak 2 (0.924 min)
94577.7
214.3
453.8
712.2
713.5
Page 1 of 2
Printed: 1/2/2019 9:23 AM